Equatorial upwelling enhances nitrogen fixation in the Atlantic Ocean

Ajit Subramaniam,[1] Claire Mahaffey,[2] William Johns,[3] and Natalie Mahowald[4]

Received 1 January 2013; revised 8 February 2013; accepted 12 February 2013.

[1] Surface waters in upwelling regions are thought to be nutrient rich and hence inhibit nitrogen fixation (diazotrophy) because diazotrophs can preferentially assimilate nitrate and ammonia instead of expending energy to fix dinitrogen. We found average nitrogen fixation rates to be two to seven times higher in the surface waters of the upwelling region of the eastern equatorial Atlantic than typically measured here during non-upwelling periods. We posit that in this region, low nitrate-phosphate ratio waters are upwelled, and an initial bloom of non-diazotrophic phytoplankton removes recently upwelled nitrate. Thereby, diazotrophy is fuelled by residual phosphate and by a combination of aeolian and upwelled sources of iron. Annually, we estimate that approximately 47 Gmol of new nitrogen is introduced by diazotrophy in upwelled waters alone and 195 Gmol N is fixed in the equatorial Atlantic region. Our findings challenge the paradigm that the highest nitrogen fixation rates occur in oligotrophic gyres and instead provide evidence of its importance in upwelling regimes where phosphate- and iron-rich waters rich are upwelled. **Citation:** Subramaniam A., C. Mahaffey, W. Johns, and N. Mahowald (2013), Equatorial upwelling enhances nitrogen fixation in the Atlantic Ocean, *Geophys. Res. Lett.*, *40*, doi:10.1002/grl.50250.

1. Introduction

[2] The equatorial Atlantic Ocean is a region of high productivity due to seasonal upwelling that brings nutrients into the euphotic zone [*Christian and Murtugudde*, 2003] and for a few months of the year covers an area greater than 2 million square kilometers. Although satellite ocean color data show enhanced surface chlorophyll concentrations during the active upwelling period from late May to September, there are few measurements of primary production in this region during this season. Also, although there have been a handful of reports quantifying diazotrophs and their diversity and rates of nitrogen fixation in the equatorial Atlantic during the nonupwelling time [*Fernández et al*., 2010; *Langlois et al*., 2005; *Montoya et al*., 2007; *Moore et al*., 2009], there is only one study published on diversity of diazotrophs during the active upwelling season [*Foster et al*., 2009], and there are no rate measurements of diazotrophy during this period. Most of our knowledge on the latitudinal distributions of the nitrogen fixing cyanobacterium, especially *Trichodesmium*, in the equatorial Atlantic has been gained through meridional transects [*Fernández et al*., 2010; *Moore et al*., 2009; *Tyrrell et al*., 2003] just before (April–May) or after (October–November) the upwelling season. These studies noted the highest *Trichodesmium* abundance and rates of nitrogen fixation between 5°N and 15°N [*Fernández et al*., 2010; *Moore et al*., 2009], with a slight southerly shift in *Trichodesmium* abundance in April. The decline or absence in nitrogen fixation south of 5°N has been attributed to the depletion of the limiting nutrient, iron, in the tropical South Atlantic, despite higher concentrations of a second limiting nutrient, phosphate, in this region [*Moore et al*., 2009]. However, these observations were made in November when there is no equatorial upwelling, and the intertropical convergence zone (ITCZ) is close to its northern most position. Others have used satellite-derived aerosol optical thickness to make an argument for considering the ITCZ as an "iron curtain" that inhibits the supply of Fe to the south of its location [*Fernández et al*., 2010].

[3] The widely held understanding of the physiology of autotrophic diazotrophs predicts low abundance and rates of nitrogen fixation in the surface waters of upwelling regions because diazotrophs could preferentially assimilate available nitrate and ammonia instead of expending energy to fix dinitrogen [*Knapp*, 2012], or they are outcompeted by other faster growing phytoplankton species. Hence, studies focused on nitrogen fixation normally do not target the equatorial band from 5°N to 6°S during the upwelling season due to the availability of nitrate, and it is considered to be out of the region receiving iron-rich dust from the Sahara [*Moore et al*., 2009].

[4] The aim of this study was to determine the spatial extent and magnitude of diazotrophic activity in the equatorial Atlantic during an active upwelling period in May and June 2009. A set of four meridional transects—at 23°W, 10°W, 0°E, and 5°E—were occupied between 6°S and 4°N. Total and size fractionated rates of nitrogen fixation were determined, along with nutrients and community structure using phytopigments. We observed increased nitrogen fixation rates in the active upwelling region and suggest a mechanism involving species succession, atmospheric forcing, and nutrient stoichiometry to explain the presence of diazotrophs in this region. Finally, we estimate the contribution of the equatorial Atlantic to basin scale rates of nitrogen fixation.

2. Methods

2.1. Nutrients, in-water Light Field, Phytoplankton Pigments, and Sea Surface Temperature Data

[5] Seawater for nutrient analyses was collected from between 6 and 12 depths from 37 Conductivity Temperature

All Supporting Information may be found in the online version of this article.

[1]Lamont Doherty Earth Observatory, Columbia University, Palisades, New York, USA.
[2]Department of Earth, Ocean and Ecological Sciences, School of Environmental Sciences, University of Liverpool, Liverpool, UK.
[3]Division of Meteorology and Physical Oceanography, Rosenstiel School of Marine and Atmospheric Science, University of Miami, Miami, Florida, USA.
[4]Department of Earth and Atmospheric Sciences, Cornell University, Ithaca, New York, USA.

Corresponding author: A. Subramaniam, Lamont Doherty Earth Observatory, Columbia University, 61 Rt 9W, Palisades, NY 10964, USA. (ajit@ldeo.columbia.edu)

0094-8276/13/10.1002/grl.50250

Depth (CTD) casts between 0 and 3000 m. Seawater was poured directly from the Niskin bottle into a precleaned HDPE bottle, immediately capped, frozen at −20°C, and analyzed at the Oregon State University COAS Chemical Analysis Laboratory using standard colorimetric techniques. Samples for phytoplankton pigments were collected from five depths and measured at the Horn Point Analytical Services Laboratory [*Van Heukelem and Thomas*, 2001]. The in-water light field was measured using a free-falling Satlantic spectroradiometer. Time series of daily sea surface temperature (SST) data at the station locations was obtained from the NCDC 0.25 Degree Daily Optimal Interpolation product, version 2.0 [*Reynolds et al*., 2007]

2.2. Nitrogen Fixation Rates

[6] Nitrogen fixation rates were measured in duplicate or triplicate at between one and six depths at pre-dawn stations only using methods outlined by Church *et al*. [2009] and Montoya *et al*. [1996]. Twenty-four-hour on-deck incubations were set up using 4.4 L precleaned polycarbonate bottles capped with silicon-septa bottle caps. Three milliliters of $^{15}N_2$ labeled gas (99 atomic %; Isotech Laboratories, Inc.) was injected through the septa of each bottle, which were shaken and shaded with neutral filters from 98% to 1% light level. Bottle contents were filtered through a GF/F or prefiltered through a 10 μm polycarbonate filter. Filters were dried at 60°C for 24 h, and the ^{15}N content was determined at the University of Hawaii using a Carlo-Erba Elemental Analyser coupled to a Thermofinnigan DeltaS. Areal rates were calculated by trapezoidal integration for each station. At three stations (23, 39, and 95), there was inadequate vertical resolution to calculate areal integrated rates.

2.3. Station Classification and Station 21 and 23 Exceptions

[7] We used the criteria of a 2°C decrease in SST from the mean value for the months of April and May to classify stations as upwelling or nonupwelling at the time of sampling. This scheme was confirmed using a Ward Hierarchical Clustering technique on SST, sea surface salinity, and mixed layer depth (MLD) measured by the CTD (Supplementary Figure S1). MLD was defined as a 0.8°C change from the surface [*Kara et al*., 2000]. Our classification scheme identified 10 stations as upwelling stations (21, 23, 37, 39, 53, 58, 62, 65, 90, and 93) in the regions identified by Kadko and Johns [2011] as upwelling based on an isotope tracer technique. The six Gulf of Guinea stations (24, 25, 29, 71, 74, and 77) were identified by their geographical coordinates (north of 0°N, east of 18°W). The three river stations (84, 95, and 96) were in the plumes of the Congo and Oguoue Rivers, as detected by the high absorption at the surface due to colored dissolved organic matter. The remaining six nonupwelling stations (5, 10, 15, 44, 49, and 50) were classified as equatorial Atlantic stations.

[8] *Foltz and McPhaden* [2010] and *Foltz et al*. [2012] identified an anomalous cooling event between March and mid May 2009 that caused an uplift of the thermocline north of 3°N at around 23°W (Supplementary Figure S2). Thus, stations 21 and 23 were not identified as upwelling stations by the change in SST, from the April to May mean value, but the cooling during the previous 40 days can clearly be seen as an anomaly from the multi-year mean for this period. Hence, we classified stations 21 and 23 as upwelling stations (Supplementary Figure S3).

2.4. Calculation of Total Dinitrogen Fixed in the Equatorial Atlantic

[9] The total dinitrogen fixed for each month was estimated as the product of the average rate calculated for each region defined as upwelling, Gulf of Guinea, and equatorial Atlantic and the area appropriate for the month. Although the area of Gulf of Guinea is constant through the year, the area of upwelling, calculated from satellite-derived SST, varies; thus, the relative contribution of new nitrogen from fixation from the upwelling and equatorial Atlantic region changes for each month (see Supplementary Table S1).

3. Results

3.1. Regional Hydrography, Nutrients, and Chlorophyll

[10] Mean SST was only marginally cooler in the upwelling (25.87°C ± 0.44°C) and river (25.53°C ± 0.28°C) stations relative to the Gulf of Guinea (28.63°C ± 0.26°C) and nonupwelling equatorial Atlantic (27.51°C ± 0.49°C), reflecting the fact that upwelled waters rarely reach the surface (Table 1). The MLD was twice as deep in the Gulf of Guinea and equatorial Atlantic (~ 40 m) compared with the upwelling and river stations (~20 m). Although the depth of the euphotic zone varied from 49 ± 9 m at the river stations to 83 ± 2 m in the Gulf of Guinea, the euphotic zone integrated chlorophyll *a* concentrations were similar across all regions (Table 1).

[11] Phosphate was measureable in surface waters at all stations sampled, with concentrations twice as high

Table 1. The Mean Sea Surface Temperature (SST, °C), Sea Surface Salinity (SSS), Mixed Layer Depth (MLD, m), Euphotic Zone Depth (Zeu, m), Areal Chlorophyll Concentration (Chl *a*, mg m^{-2}), Surface Phosphate, Nitrate and Silicate Concentrations (μmol L^{-1}), Bulk Areal Nitrogen Fixation Rates, and Percentage Contribution from the <10 μm Size Fraction

Parameter	Upwelling	Gulf of Guinea	Equatorial Atlantic	River
SST (°C)	25.87 ± 0.44 (9)	28.63 ± 0.24 (6)	27.51 ± 0.49 (6)	25.53 ± 0.28 (3)
SSS	35.58 ± 0.14 (9)	34.60 ± 0.13 (6)	35.52 ± 0.09 (6)	34.57 ± 0.26 (3)
MLD (m)	25 ± 2 (9)	41 ± 5 (6)	41 ± 4 (6)	21 ± 3 (3)
Zeu (m)	67 ± 2 (7)	83 ± 2 (6)	80 ± 4 (5)	49 ± 9 (2)
Areal Chl *a* (mg m^{-2})	26 ± 2 (9)	27 ± 2 (6)	26 ± 1 (6)	23 ± 7 (3)
Surface phosphate (μmol L^{-1})	0.18 ± 0.03 (15)	0.09 ± 0.01 (15)	0.11 ± 0.01 (6)	0.18 ± 0.01 (3)
Surface nitrate (μmol L^{-1})	0.20 ± 0.02 (11/15)	0.21 ± 0.01 (4/15)	0.13 ± 0.01 (4/6)	Below limits of detection
Surface silicate (μmol L^{-1})	1.57 ± 0.15 (15)	1.52 ± 0.3 (15)	1.15 ± 0.15 (6)	4.58 ± 1.3 (3)
Areal N_2 fixation (μmol m^{-2} day^{-1})	134 ± 55 (9) 15 to 424	159 ± 24 (6) 44 to 205	60 ± 20 (6) 23 to 154	63 ± 5 (3) 53 to 69
% areal N_2 fixation <10 μm	48 ± 10 (9)	23 ± 5 (6)	45 ± 4 (6)	64 ± 27 (3)

Mean ± 1 standard error of parameters for each of the station types is presented. The number of stations for each type is in parenthesis.

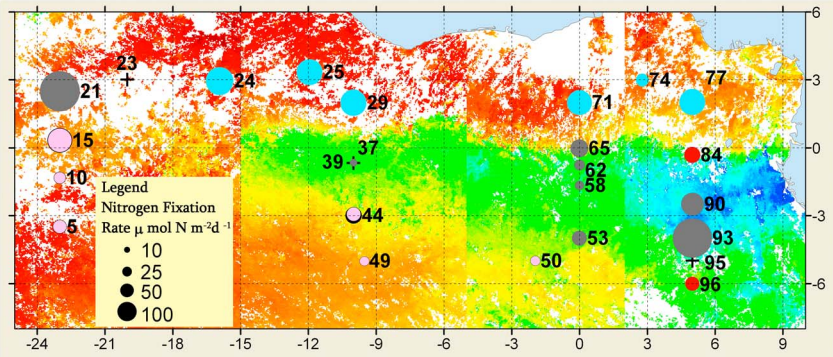

Figure 1. Station locations superimposed on 8-day composites of satellite-derived sea surface temperature (SST, °C). The map is made up of four 8-day composites, corresponding to stations sampled during those 8 days. Area of the circle for each station is proportional to the areal rate of nitrogen fixation (μmol N m^{-2} day^{-1}). The color of the circles indicates the station type (equatorial Atlantic—ATL [pink], upwelling—UPW [black], Gulf of Guinea—GOG [blue], river plume—RIV [red]). Stations indicated with + are those where an areal integrated rate could not be calculated.

in the upwelling stations (0.18 ± 0.03 μM) and river stations (0.18 ± 0.01 μM) compared with the Gulf of Guinea (0.09 ± 0.01 μM) and equatorial Atlantic (0.11 ± 0.01 μM, Table 1).

[12] Nitrate was measurable in surface waters at 11 of 15 upwelling (0.20 ± 0.02 μM), at 4 of 15 Gulf of Guinea (0.21 ± 0.01 μM), and at 4 of 6 equatorial Atlantic (0.13 ± 0.01 μM) stations but was below the limits of detection (0.1 μM) in the river stations (Table 1). Silicate was measurable in surface waters in all regions (Table 1). The surface water nitrate-phosphate ratio was between 1 and 2 for all regions, whereas the depth averaged nitrate-phosphate ratio between 100 and 300 m was 13.6 ± 1.1, $n = 156$ (Supplementary Figure S4). We estimated that upwelling stations along the 10°W transect (37–41), the 0°E transect (53–65), and the 5°E transect (86–93) were visited approximately 3, 8, and 18 days after the onset of upwelling, respectively (Figure 2a).

3.2. Rates of Nitrogen Fixation

[13] Euphotic zone integrated rates of nitrogen fixation were enhanced in upwelled waters (134 ± 55 μmol m^{-2} day^{-1}, ranging from 15 to 424 μmol m^{-2} day^{-1}) relative to average rates observed in the nonupwelling Atlantic (60 ± 20 μmol m^{-2} day^{-1}, ranging from 23 to 154 μmol m^{-2} day^{-1}) and the river-influenced stations (63 ± 5 μmol m^{-2} day^{-1}, ranging from 53 to 69 μmol m^{-2} day^{-1}) (Figure 1, Table 1).

[14] Although rates of nitrogen fixation were similar for the Gulf of Guinea (159 ± 24 μmol m^{-2} day^{-1}) and the upwelling stations (Table 1), the relative contribution of the < 10 μm size fraction to total nitrogen fixation was significantly higher in the upwelling (48 ± 10%) compared with the Gulf of Guinea stations (23 ± 5%) ($p = 0.01$, Table 1). The large range in nitrogen fixation rates in the upwelling stations was due to a west to east gradient that we attribute to "aging" of upwelled waters or days since the onset of upwelling (Figure 2b). Maximum areal rates of nitrogen fixation, greater than 400 μmol m^{-2} day^{-1}, were observed at upwelling stations where the onset had occurred at least 15 days before sampling. MLDs were shallowest at these stations, which have been invoked to support enhanced diazotrophic activity (5, 18). Diazotrophs in the <10 μm size

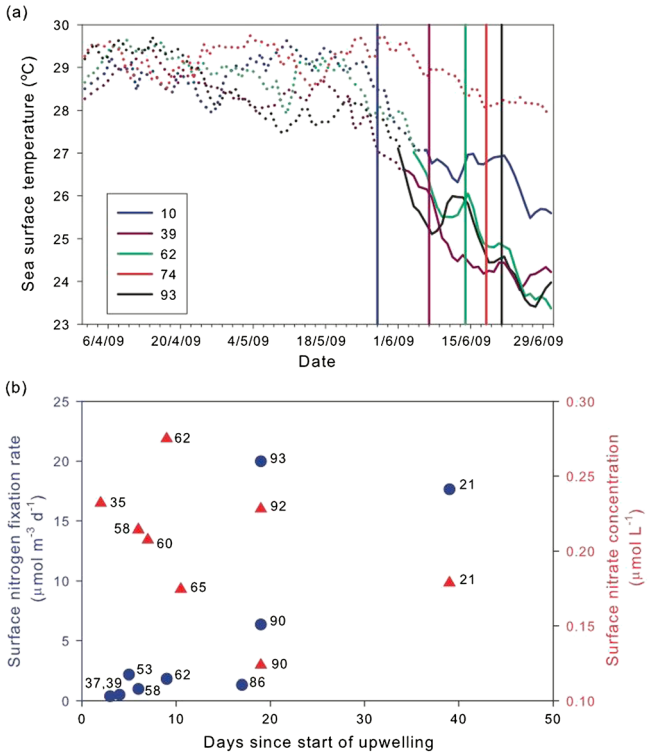

Figure 2. (A) Time series of sea surface temperature (SST, °C) at stations 10, 39, 62, 74, and 93 corresponding to the 23°W, 10°W, 0°E, 2°E, and 5°E sections respectively. The solid lines indicate times of active upwelling, estimated as initiating when the SST drops by 2°C from the average for the period 1 April to 15 May 2009. The vertical solid lines indicate when that station was sampled. The time series from station 74 in the Gulf of Guinea is also shown for comparison as a nonupwelling station. Note the exception for station 21 on the 23°W transect in Supplementary Figure S3. (B) Surface nitrogen fixation rates (μmol m^{-3} day^{-1}, left axis, blue symbols) measured at the upwelling stations plotted against the days since start of upwelling or "age" of upwelling, calculated from change in SST as shown in Figure 2a. Surface nitrate concentrations (μmol L^{-1}, red triangles and axis) were detectable (limit of detection = 0.1 μmol L^{-1}) for the same stations.

fraction contributed 67% of the surface nitrogen fixation at 10°W but only 19% and 41% at the 0°E and 5°E stations, respectively, implying an increased contribution of larger diazotrophs to total nitrogen fixation in the east where the onset of upwelling had occurred earlier.

3.3. Community Structure

[15] The zonal gradient was also evident in the phytoplankton community composition. Concentrations of diagnostic pigments [*Vidussi et al*. 2001] indicative of prymnesiophytes (containing chlorophyll *c* and 19′-hexanoyloxyfucoxanthin) were higher at the 10°W stations (9.7 and 5.8 mg m^{-2}, respectively) relative to 0°E (7.6 and 4.6 mg m^{-2}, respectively) or 5°E (5.5 and 2.7 mg m^{-2}, respectively) upwelling stations (Supplementary Figure S5). Although pigments associated with cyanobacteria and prochlorophytes (zeaxanthin and chlorophyll *b*) dominated in surface waters at all stations (61% ± 4% to 74% ± 2% of total diagnostic pigments), the relative contribution by pigments associated with diatoms and dinoflagellates (peridinin and fucoxanthin) was significantly greater at the upwelling stations (11% ± 2%) than at the Gulf of Guinea or equatorial Atlantic stations (~7% ± 1%) ($p = 0.04$ for both).

3.4. Regional Rates of Nitrogen Fixation

[16] If we assume the 26°C isotherm to define the boundary of the cold tongue between May and September in the box bounded by 5°N and 6°S, 52.5°W, and 12.5°E and use the average nitrogen fixation rate of 134 ± 55 μmol N m^{-2} day^{-1} estimated for waters influenced by upwelling, we calculate the annual input of new nitrogen from nitrogen fixation to be 47 ± 19 Gmol N in the upwelling region. If we assume an average rate of nitrogen fixation of 60 μmol N m^{-2} day^{-1} for the entire equatorial Atlantic during months when there is no upwelling (January–April, October–December) and use the same rate to estimate the contribution of the nonupwelling region of the Atlantic during the upwelling period (May–September), we estimate 75 ± 25 Gmol N per year. The annual input from the Gulf of Guinea using the average rate of 159 ± 24 μmol m^{-2} day^{-1} amounts to an additional 73 ± 11 Gmol N. Thus, we calculate that the equatorial Atlantic (5°N to 6°S, 65°W to 15°E) contributes 195 ± 56 Gmol N annually in new nitrogen from nitrogen fixation, approximately 13% of the average of current estimates that range from 1400 to 2000 Gmol N [*Capone et al*., 2005; *Gruber and Sarmiento*, 1997; *Moore et al*., 2009] for the entire North Atlantic Ocean (Supplementary Table S1). These estimates are conservative in that recent studies [*Mohr et al*., 2010] suggest that $^{15}N_2$ gas uptake techniques might underestimate nitrogen fixation rates.

4. Discussion

[17] We postulate that although phosphate may limit nitrogen fixation rates in the tropical North Atlantic stations [*Sanudo-Wilhelmy et al*., 2001] and iron may limit nitrogen

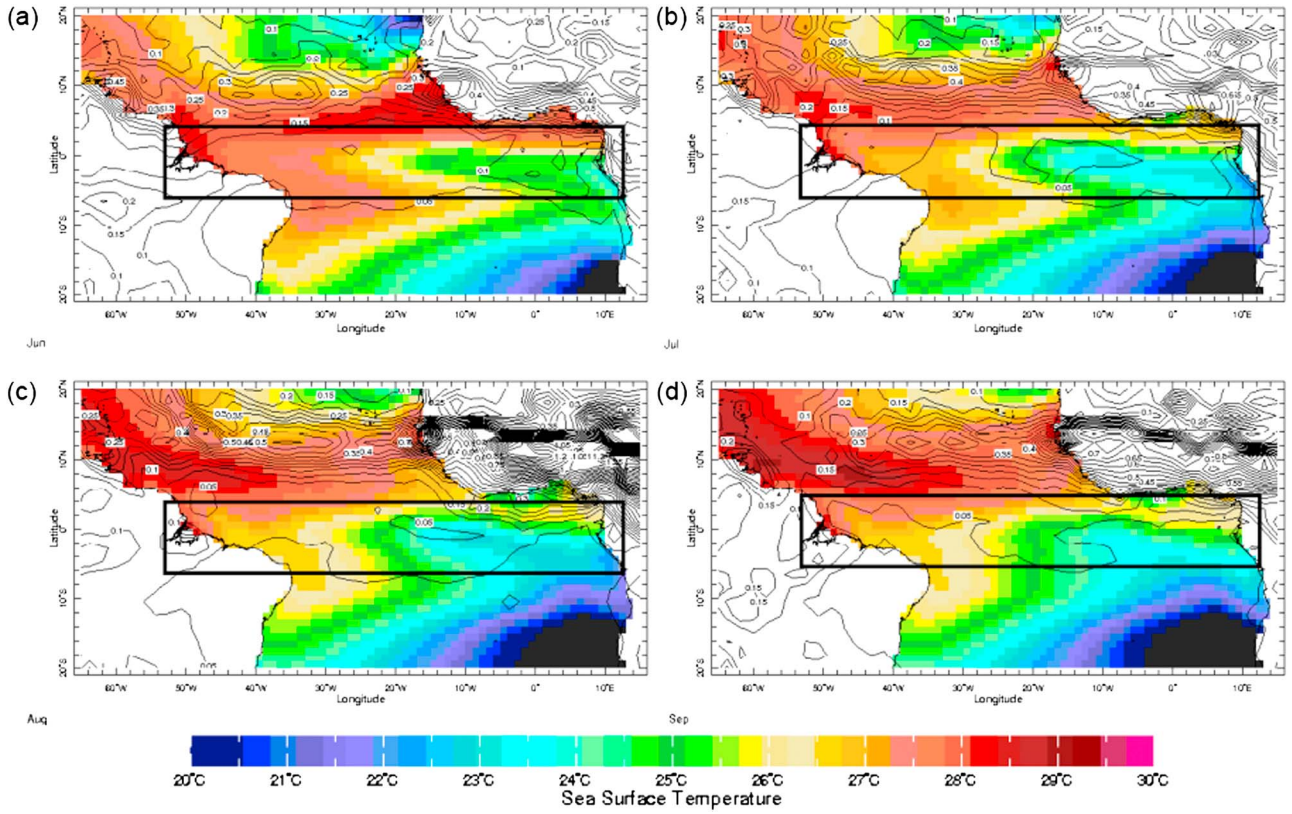

Figure 3. Dissolved iron (Fe) deposition rates (ng m^{-2} s^{-1}) modeled by *Luo et al*. [2008] shown as contours overlaid on Reynolds and Smith OI v2 climatological SST (°C) for the months (A) June, (B) July, (C) August, and (D) September. The southernmost contour shown (0.05 ng m^{-2} s^{-1}) corresponds to a deposition rate for soluble Fe (II) of 77 nmol Fe m^{-2} day^{-1}. The box indicates the area used to calculate the total nitrogen fixed (Supplementary Table S1).

fixation in the tropical South Atlantic stations [*Fernández et al*., 2010; *Moore et al*., 2009], both these limitations are alleviated in the upwelling stations sampled in this study. This results in nitrogen fixation rates that far exceed (up to 400 μmol m^{-2} day^{-1}) those typically measured in the subtropical gyre (up to 200 μmol m^{-2} day^{-1}, 2, 5) or in other upwelling regions (85 μmol m^{-2} day^{-1} [*Sohm et al*., 2011]). The mechanisms supplying phosphate and iron differ. The drawdown of nitrate by nondiazotrophs in upwelled waters (Figure 2b) with a nitrate-phosphate ratio 16:1 leaves "excess" surface phosphate to fuel diazotrophy. The extent of the alleviation of phosphorus limitation is sensitive to the duration of upwelling or "age" of upwelled waters and requires a succession of phytoplankton species that are able to assimilate nitrate and phosphate at a ratio close to 16:1. Indeed, such a conceptual model has been described by *Karl and Letelier* [2008]. Also, there is good observational and modeled evidence that this region may not be iron limited during the upwelling period. As well as supplying phosphate, upwelling may supply iron. Shipboard measurements report iron concentrations in excess of 1.4 nM at 100 m (23) and up to 0.8 nM in surface waters during upwelling in this region (22). *Luo et al*. [2008] modeled the deposition of soluble iron (II) in the world's ocean, including both cloud and combustion processes, and found that biologically relevant deposition rates extend south of the ITCZ during the upwelling period (Figure 3). The 0.05 ng m^{-2} s^{-1} contour from their model, corresponding to a deposition rate for soluble iron (II) of 77 nmol m^{-2} day^{-1}, extends to approximately 5°S through much of the upwelling period. If we assume that this supply is distributed over the mixed layer (25 m), this would provide 3.1 nmol soluble iron (II) per day.

[18] Perhaps it should be unsurprising to find diazotrophs and enhanced nitrogen fixation rates in regions of active upwelling. Model studies in the Atlantic Ocean show enhanced nitrogen fixation rates in the equatorial Atlantic [*Monteiro et al*. 2010; *Hood et al*., 2004]. In particular, *Monteiro et al*. [2010] predicted the highest nitrogen fixation rates to occur in equatorial Atlantic between May and September, the period of active upwelling, which may be attributed to a rapid response by unicellular diazotrophs to iron inputs [*Benavides et al*., 2013]. In addition, there is growing evidence from field observations and laboratory studies that nitrogen fixation continues, albeit at a reduced rate, during long-term exposure to relatively high concentrations of nitrate (>5 μM, [*Fernandez et al*., 2011; *Knapp*, 2012; *Knapp et al*., 2012; *Sohm et al*., 2011]). Laboratory studies involving batch cultures of *Trichodesmium* and *Crocosphaera*, two common diazotrophs, under varying (but environmentally relevant) nitrate-to-phosphate ratios reveal that excess nitrate (relative to phosphate) reduces the rates of nitrogen fixation whereas excess phosphate (relative to nitrate) increases the number of cells (due to the physiological requirement of phosphorus for DNA), and not the per cell rates of nitrogen fixation, resulting in an overall increase in the volumetric rate of nitrogen fixation. *Sohm et al*. [2011] reported maximum nitrogen fixation rates of 7.5 nmol L^{-1} day^{-1} in surface waters of the Benguela upwelling region where nitrate concentrations were 21 μM. We found nitrogen fixation rates in excess of 5 nmol L^{-1} day^{-1} at several upwelling and Gulf of Guinea stations with maximal rates approaching 20 nmol L^{-1} day^{-1} at some upwelling stations, but surface nitrate concentrations did not exceed 0.3 μM. Thus, it is possible that the activity of diazotrophs is dependent on the local upwelling regime, and the magnitude of nitrogen fixation is time varying.

Summary

[19] The results presented adds to a growing body of evidence [*Knapp*, 2012; *Knapp et al*., 2012; *Sohm et al*., 2011] that not only challenges the paradigm that the highest nitrogen fixation rates occur in oligotrophic gyres but also our current understanding of carbon and nitrogen cycle dynamics in upwelling regions. We provide evidence that emphasizes its importance in upwelling regimes where low nitrate-phosphate waters are upwelled and there is significant atmospheric deposition of iron. Although observations presented here are focused on the tropical Atlantic, it is likely that other regions with similar upwelling regimes, such as in the Indian Ocean and marginal seas (e.g., South China Sea), support extensive diazotroph communities. However, field campaigns are required to further investigate the timescales of response between the onset of upwelling, succession of species and depletion of nutrients including iron, to fully understand the consequences to nitrogen and carbon cycle.

[20] **Acknowledgments.** This work was supported by the NASA Ocean Biology and Biogeochemistry (grant no. NNG05GR37G to AS) and the National Science Foundation (grant no. OCE 0623552 to WJ). The authors thank Alexey Kaplan for providing the interpolated daily SST data and Andy Juhl, Gregory Foltz, and Ric Williams for their constructive contribution and feedback. AS and CM contributed equally to this work. This is LDEO contribution # 7664.

References

Benavides, M., J. Arístegui, N. S. R. Agawin, J. López Cancio, and S. Hernández-León (2013), Enhancement of nitrogen fixation rates by unicellular diazotrophs vs. Trichodesmium after a dust deposition event in the Canary Islands, *Limnol. Oceanogr.*, *58*(1), 267–275.

Capone, D., J. A. Burns, J. P. Montoya, A. Subramaniam, C. Mahaffey, T. Gunderson, A. F. Michaels, and E. J. Carpenter (2005), Nitrogen fixation by *Trichodesmium* spp.: An important source of new nitrogen to the tropical and subtropical North Atlantic Ocean, *Global Biogeochem. Cycles*, *19*(GB2024), doi:10.1029/2004GB002331.

Christian, J. R., and R. Murtugudde (2003), Tropical Atlantic variability in a coupled physical-biogeochemical ocean model, *Deep-Sea Research II*, *50*, 2947–2969.

Church, M. J., C. Mahaffey, R. M. Letelier, R. Lukas, J. P. Zehr, and D. M. Karl (2009), Physical forcing of nitrogen fixation and diazotroph community structure in the North Pacific subtropical gyre, *Glob. Biogeochem. Cycles*, *23*(GB2020), doi:10.1029/2008GB003418.

Fernandez, C., L. Farias, and O. Ulloa (2011), Nitrogen Fixation in Denitrified Marine Waters, *PLoS One*, *6*(6), e20539.

Fernández, A., B. Mouriño-Carballido, A. Bode, M. Varela, and E. Marañón (2010), Latitudinal distribution of *Trichodesmium* spp. and N_2 fixation in the Atlantic Ocean, *Biogeosciences*, *7*(10), 3167–3176.

Foltz, G. R., and M. J. McPhaden (2010), Abrupt equatorial wave-induced cooling of the Atlantic cold tongue in 2009, *Geophys. Res. Lett.*, *37*, L24605, doi:10.1029/2010GL045522.

Foltz, G. R., M. J. McPhaden, and R. Lumpkin (2012), A Strong Atlantic Meridional Mode Event in 2009: The Role of Mixed Layer Dynamics, *J. Climate*, *25*(1), 363–380.

Foster, R. A., A. Subramaniam, and J. P. Zehr (2009), Distribution and activity of diazotrophs in the Eastern Equatorial Atlantic, *Environ. Microbiol.*, *11*(4), 741–750.

Gruber, N., and J. L. Sarmiento (1997), Global patterns of marine nitrogen fixation and denitrification, *Global Biogeochem. Cycles*, *11*(2), 235–266.

Hood, R. R., V. J. Coles, and D. G. Capone (2004), Modeling the distribution of Trichodesmium and nitrogen fixation in the Atlantic Ocean, *Journal of Geophysical Research, C, Oceans*, *109*(6), doi:10.1029/2002JC001753.

Kadko, D., and W. Johns (2011), Inferring upwelling rates in the equatorial Atlantic using 7Be measurements in the upper ocean, *Deep-Sea Res. I Oceanogr. Res. Pap.*, *58*(6), 647–657.

Kara, A. B., P. A. Rochford, and H. E. Hurlburt (2000), An optimal definition for ocean mixed layer depth, *Journal of Geophysical Research-Oceans*, *105*(C7), 16803–16821.

Karl, D. M., and R. M. Letelier (2008), Nitrogen fixation-enhanced carbon sequestration in low nitrate, low chlorophyll seascapes, *Mar. Ecol. Prog. Ser.*, *364*, 257–268.

Knapp, A. N. (2012), The sensitivity of marine N_2 fixation to dissolved inorganic nitrogen, *Front. Microbiol.*, *3*(374), 1–14.

Knapp, A. N., J. Dekaezemacker, S. Bonnet, J. A. Sohm, and D. G. Capone (2012), Sensitivity of *Trichodesmium* and *Crocosphaera* abundance and N_2 fixation rates to varying NO_3 and PO_4 concentrations in batch cultures, *Aquat. Microb. Ecol.*, *66*, 223–236.

Langlois, R. J., J. LaRoche, and P. A. Raab (2005), Diazotrophic Diversity and Distribution in the Tropical and Subtropical Atlantic Ocean, *Appl. Environ. Microbiol.*, *71*, 7910–7919.

Luo, C., N. Mahowald, T. Bond, P. Y. Chuang, P. Artaxo, R. Siefert, Y. Chen, and J. Schauer (2008), Combustion iron distribution and deposition, *Global Biogeochem. Cycles*, *22*(1).

Mohr, W., T. Grosskopf, D. W. R. Wallace, and J. LaRoche (2010), Methodological Underestimation of Oceanic Nitrogen Fixation Rates, *PLoS One*, *5*(9).

Monteiro, F. M., M. J. Follows, and S. Dutkiewicz (2010), Distribution of diverse nitrogen fixers in the global ocean, *Global Biogeochem. Cycles*, *24*(3).

Montoya, J. P., M. Voss, and D. G. Capone (2007), Spatial variation in N-2-fixation rate and diazotroph activity in the Tropical Atlantic, *Biogeosciences*, *4*(3), 369–376.

Montoya, J. P., M. Voss, P. Kaehler, and D. G. Capone (1996), A simple, high precision tracer assay for dinitrogen fixation, *Appl. Environ. Microbiol.*, *62*, 986–993.

Moore, C. M., *et al*. (2009), Large-scale distribution of Atlantic nitrogen fixation controlled by iron availability, *Nat. Geosci.*, *2*(12), 867–871.

Reynolds, R. W., T. M. Smith, C. Liu, D. B. Chelton, K. S. Casey, and M. G. Schlax (2007), Daily High-Resolution-Blended Analyses for Sea Surface Temperature, *J. Climate*, *20*(22), 5473–5496.

Sanudo-Wilhelmy, S. A., A. B. Kustka, C. J. Gobler, D. A. Hutchins, M. Yang, K. Lwiza, J. Burns, D. G. Capone, J. A. Raven, and E. J. Carpenter (2001), Phosphorus limitation of nitrogen fixation by *Trichodesmium* in the central Atlantic Ocean, *Nature*, *411*(6833), 66–69.

Sohm, J. A., J. A. Hilton, A. E. Noble, J. P. Zehr, M. A. Saito, and E. A. Webb (2011), Nitrogen fixation in the South Atlantic Gyre and the Benguela Upwelling System, *Geophy. Res. Lett.*, *38*(L16608), doi:10.1029/2011GL048315.

Tyrrell, T., E. Maranon, A. J. Poulton, A. R. Bowie, D. S. Harbour, and E. M. S. Woodward (2003), Large-scale latitudinal distribution of Trichodesmium spp. in the Atlantic Ocean, *J. Plankton Res.*, *25*, 405–416.

Van Heukelem, L., and C. S. Thomas (2001), Computer-assisted high-performance liquid chromatography method development with applications to the isolation and analysis of phytoplankton pigments, *J. Chromatogr. A.*, *9*(910), 31–49.

Vidussi, F., H. Claustre, B. B. Manca, A. Luchetta, and J. C. Marty (2001), Phytoplankton pigment distribution in relation to upper thermocline circulation in the eastern Mediterranean Sea during winter, *J. Geophys. Res.*, *106*(C9), 19,939–919,956.

Supplementary Information

Supplementary Figure and Table Legends

Supplementary Figure S1. (a) Dendrogram of the Wards Means Hierarchical Clustering of stations based on sea surface temperature (°C), surface salinity, and mixed layer depth (m). The upwelling stations (green) cluster together. (b) Stations plotted on a TS plot showing the grouping of the different station types; Atlantic (pink), Upwelling (black), Gulf of Guinea (blue) and River-influenced (red).

Supplementary Figure S2. (a) Ekman pumping Jan-Apr 2009. (b) Ekman pumping Jan-Apr climatology. (c) SST anomaly and Wind speed in 2009 for the box 2°N-12°N, 15°W-45°W. (d) Ekman pumping in 2009, climatological Ekman pumping, and depth of the 20°C isoterm anomaly for the same box. Note the strong Ekman pumping in March-May that ends just before station 21 was sampled.

Supplementary Figure S3. Time series of SST anomalies (°C) at stations 15 (blue), 21 (Red), and 24 (purple), showing that station 21 was influenced by an upwelling event that ended just before it was sampled. The vertical lines indicate when each station was sampled.

Supplementary Figure S4. Average profiles of Temperature (°C), Salinity, Chlorophyll (mg m-3), and N:P stoichiometry (mol:mol) for the four station types: Atlantic (pink), Upwelling (black), Gulf of Guinea (blue) and River-influenced (red). Note the shallower thermocline and chlorophyll maximum at the Upwelling stations.

Supplementary Figure S5. Depth integrated concentrations of chlorophyll *c* and 19′-hexanoyloxyfucoxanthin, marker pigments for prymnesiophytes shown as a function of days since the upwelling started. Note the decrease in concentrations of these pigments with time supports the idea that prymnesiophytes were the first to respond to the injection of new nutrients at the onset of upwelling but this trend is not statistically significant ($p < 0.05$).

Supplementary Table S1. Monthly estimates of the area of active upwelling and associated rates of nitrogen fixation for the region extending from 5°N-6°N, 12.5°E to 52.5°W in the tropical Atlantic.

Supplementary Table S1. Monthly estimates of the area of active upwelling and associated rates of nitrogen fixation for the region extending from 5°N-6°N, 12.5°E to 52.5°W in the tropical Atlantic.

			Nitrogen fixed per month (10^9 mol N $month^{-1}$)		
Month	Days per month	Area of active upwelling (x 10^{12} m^2)[a]	Active upwelling region	Non-upwelling equatorial Atlantic[b]	Gulf of Guinea[c]
January	31	0	0	8.2	6.2
February	28	0	0	7.4	5.6
March	31	0	0	8.2	6.2
April	30	0	0	7.9	6.0
May	31	0.173	0.7	7.9	6.2
June	30	1.872	7.5	4.6	6.0
July	31	2.762	11.5	3.1	6.2
August	31	3.522	14.6	1.6	6.2
September	30	3.225	13.0	2.1	6.0
October	31	0	0	8.2	6.2
November	30	0	0	7.9	6.0
December	31	0	0	8.2	6.1
Total annual nitrogen fixed per region (x 10^9 mol N)			47	75	73
Total annual nitrogen fixed, Equatorial Atlantic (x 10^9 mol N)[d]			195		
Percentage contribution of upwelling to Equatorial Atlantic[e]			24% (49%)		
Percentage contribution of Equatorial Atlantic to total N. Atlantic[f]			13%		

[a] The monthly area of upwelling is calculated as the area with SST lower than 26°C for the months May-September within the region 5°N-6°S, 12.5°E to 52.5°W.

[b] The area of the non-upwelling Equatorial Atlantic is calculated as the sum of the areas within 5°N-6°S, 52.5°W-18°W and 0°N-6°S, 18°W-12.5°E for the months without upwelling (Jan-Apr and Oct-Dec). During the upwelling months, the area of active upwelling is subtracted from this total area. The total nitrogen fixed is calculated by multiplying the area by the number of days in the month and the average fixation rate of 60 ± 20 μmol m^{-2} d^{-1}.

[c] The area of the Gulf of Guinea is calculated as the area within the region 5°N-0°N, 18°W-12.5°E. The total nitrogen fixed is calculated by multiplying the area by the number of days in the month and the average fixation rate of 159 ± 24 μmol m^{-2} d^{-1}.

[d] Total annual nitrogen fixed is calculated as the sum of nitrogen fixed in the upwelling region, the non-upwelling region, and the Gulf of Guinea.

[e] The upwelling region contributes 24% of the total nitrogen fixed annually but 51% of the nitrogen fixed during the upwelling months.

[f] We use an average nitrogen fixation rate of 1520 x 10^9 mol N per year for the whole N. Atlantic nitrogen fixation from Moore et al 2009 to calculate 13% as (193/1520)*100.

(a)

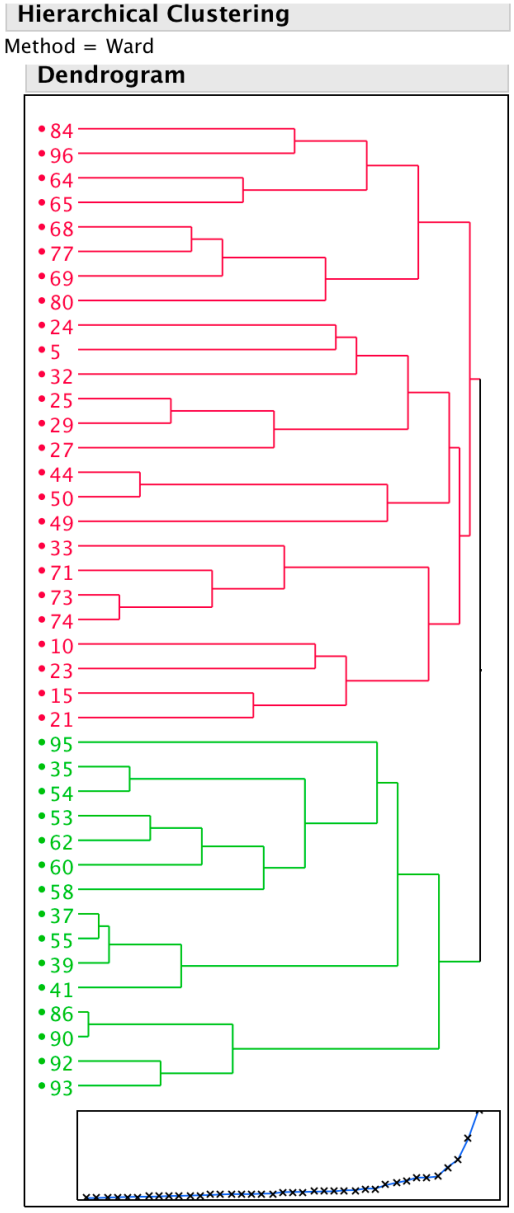
Hierarchical Clustering
Method = Ward
Dendrogram
84
96
64
65
68
77
69
80
24
5
32
25
29
27
44
50
49
33
71
73
74
10
23
15
21
95
35
54
53
62
60
58
37
55
39
41
86
90
92
93

(b)

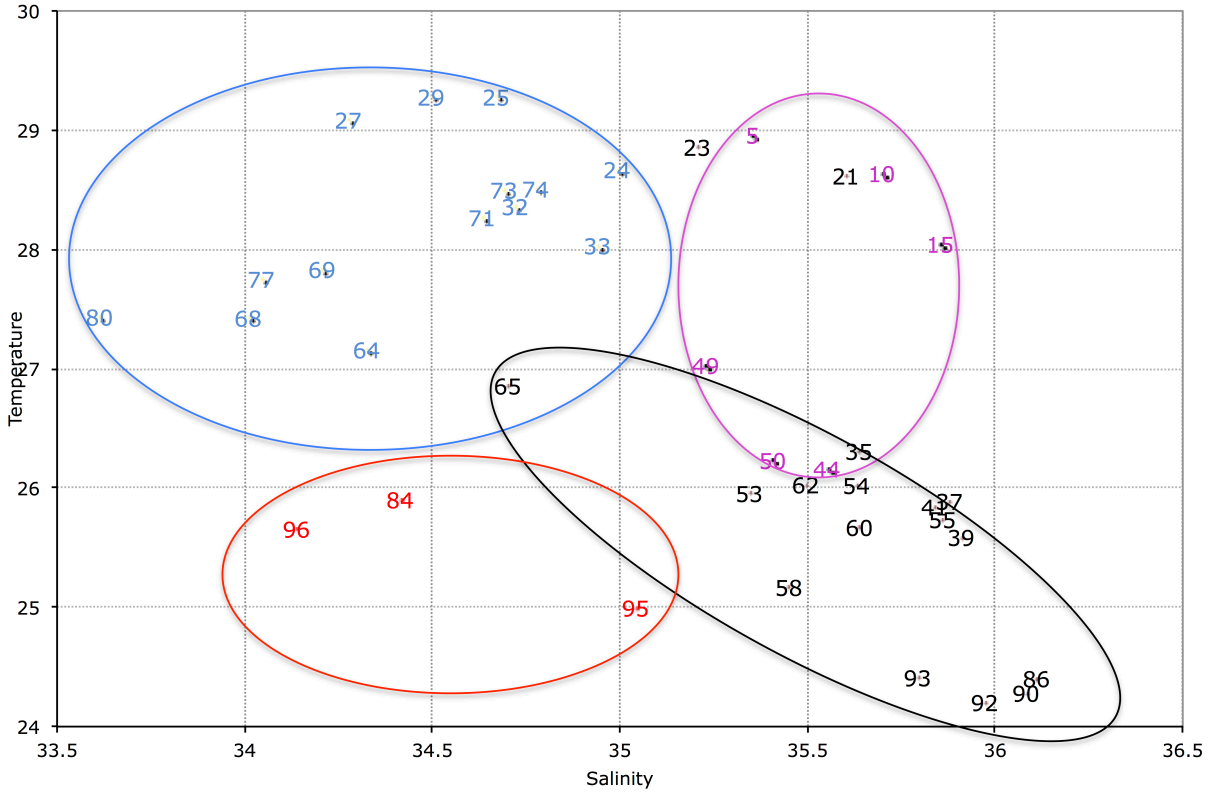
Temperature
Salinity
30
29
28
27
26
25
24
33.5
34
34.5
35
35.5
36
36.5
29
25
27
24
23
5
21
10
73
74
71
32
33
15
77
69
80
68
64
49
65
50
44
35
53
62
54
84
37
55
60
39
96
58
95
93
86
92
90

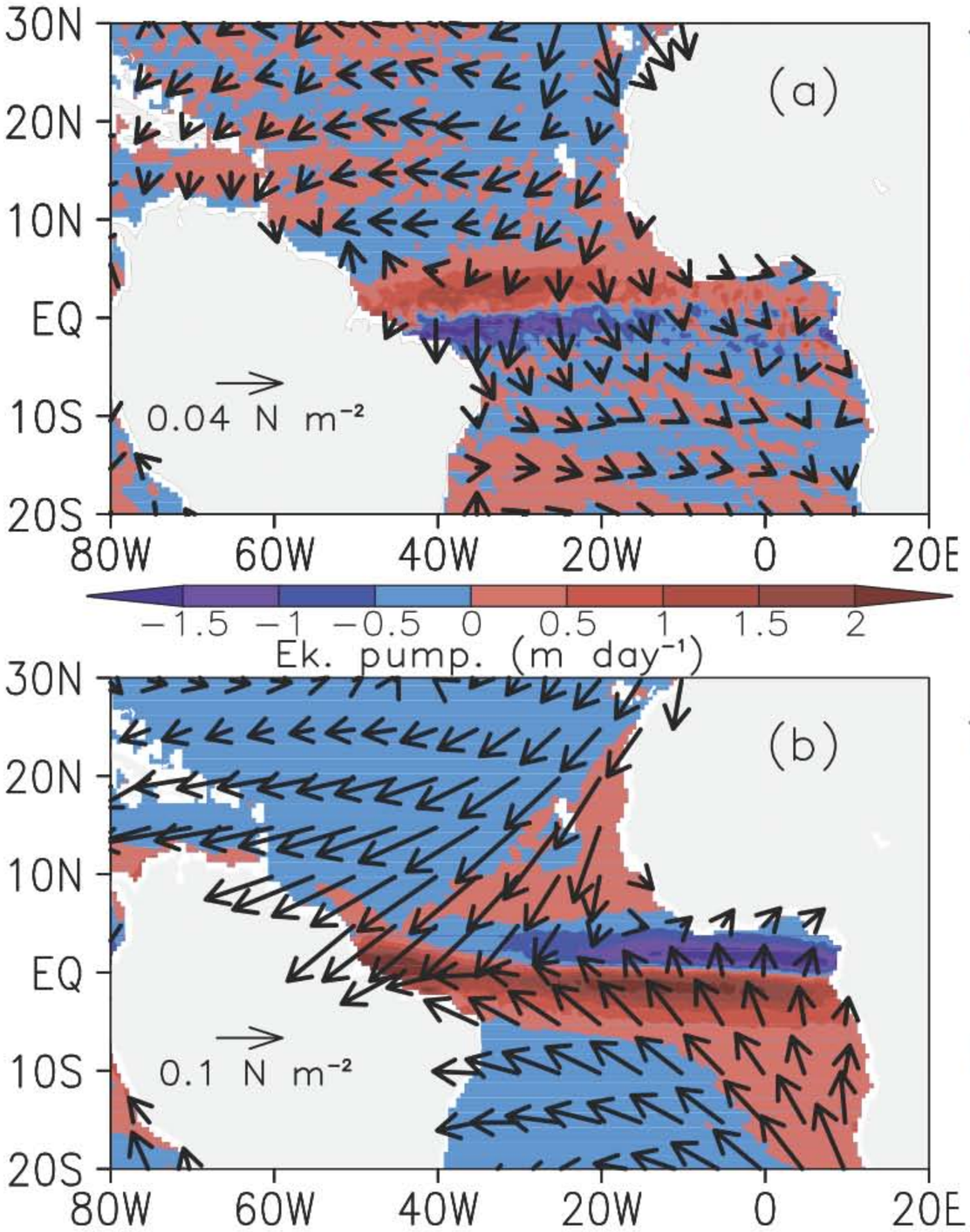
(a)
30N
20N
10N
EQ
10S
20S
80W
60W
40W
20W
0
20E
0.04 N m⁻²
−1.5 −1 −0.5 0 0.5 1 1.5 2
Ek. pump. (m day⁻¹)
(b)
0.1 N m⁻²

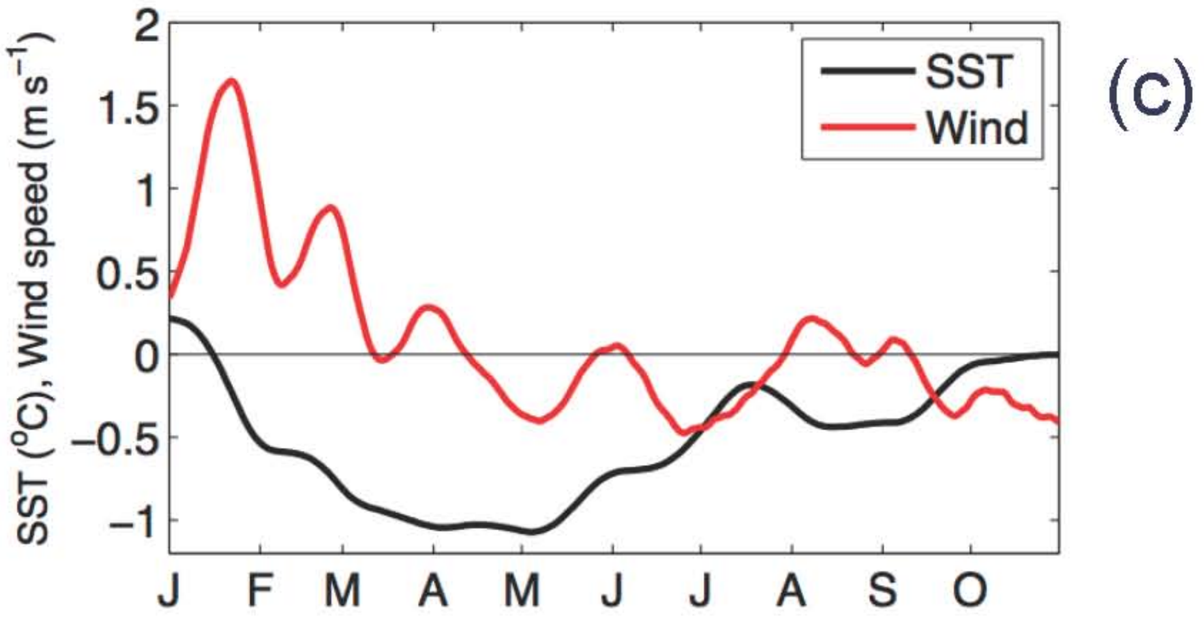
SST (°C), Wind speed (m s⁻¹)
2
1.5
1
0.5
0
−0.5
−1
SST
Wind
J F M A M J J A S O
(c)

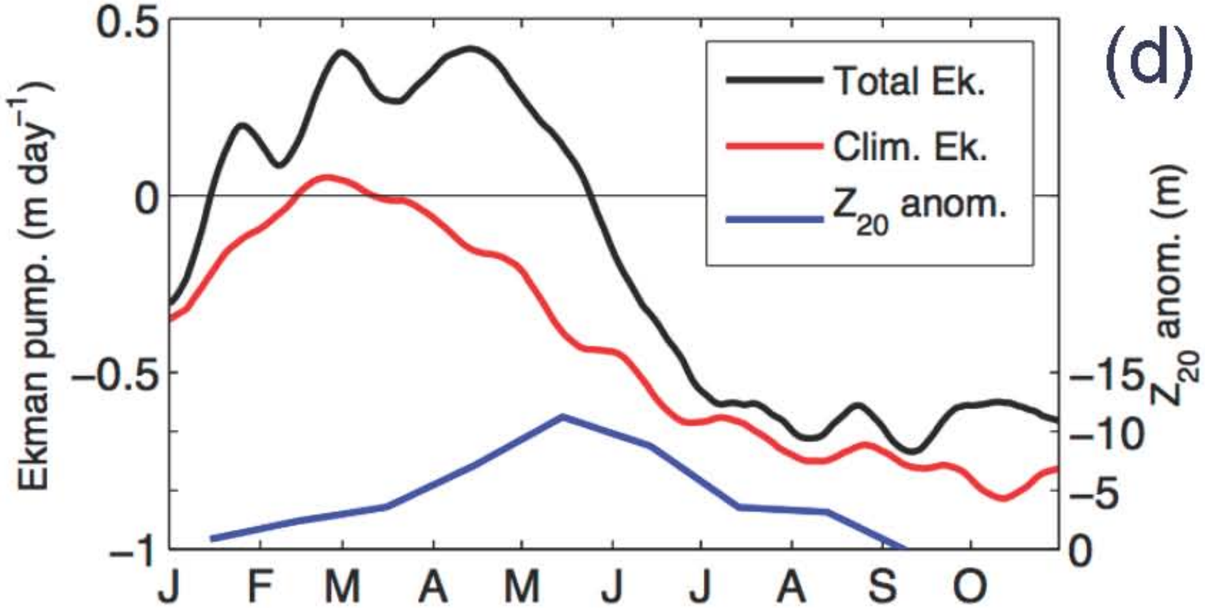
Ekman pump. (m day⁻¹)
0.5
0
−0.5
−1
Total Ek.
Clim. Ek.
Z20 anom.
Z20 anom. (m)
−15
−10
−5
0
J F M A M J J A S O
(d)

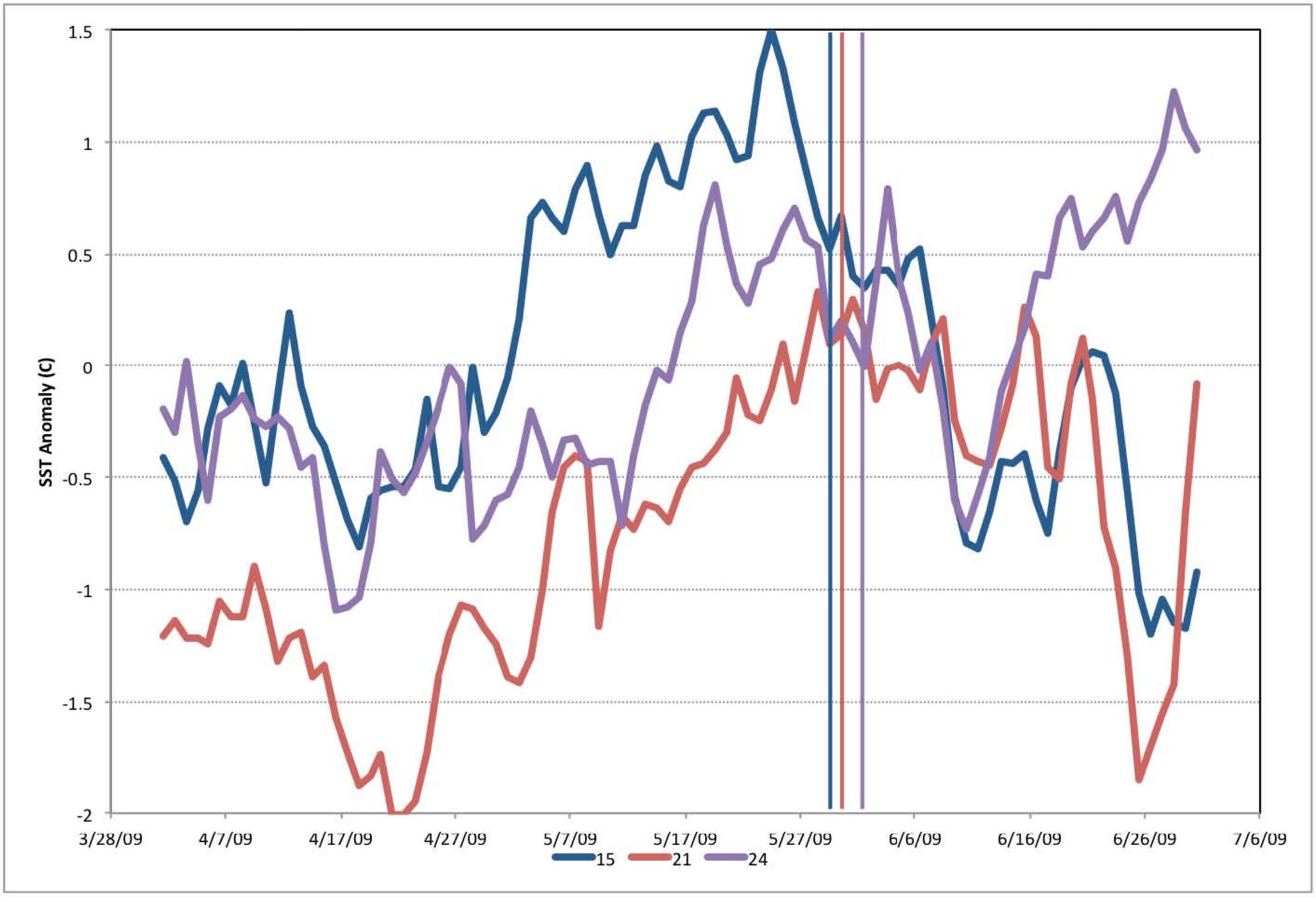
1.5
1
0.5
0
-0.5
-1
-1.5
-2
SST Anomaly (C)
3/28/09
4/7/09
4/17/09
4/27/09
5/7/09
5/17/09
5/27/09
6/6/09
6/16/09
6/26/09
7/6/09
15
21
24

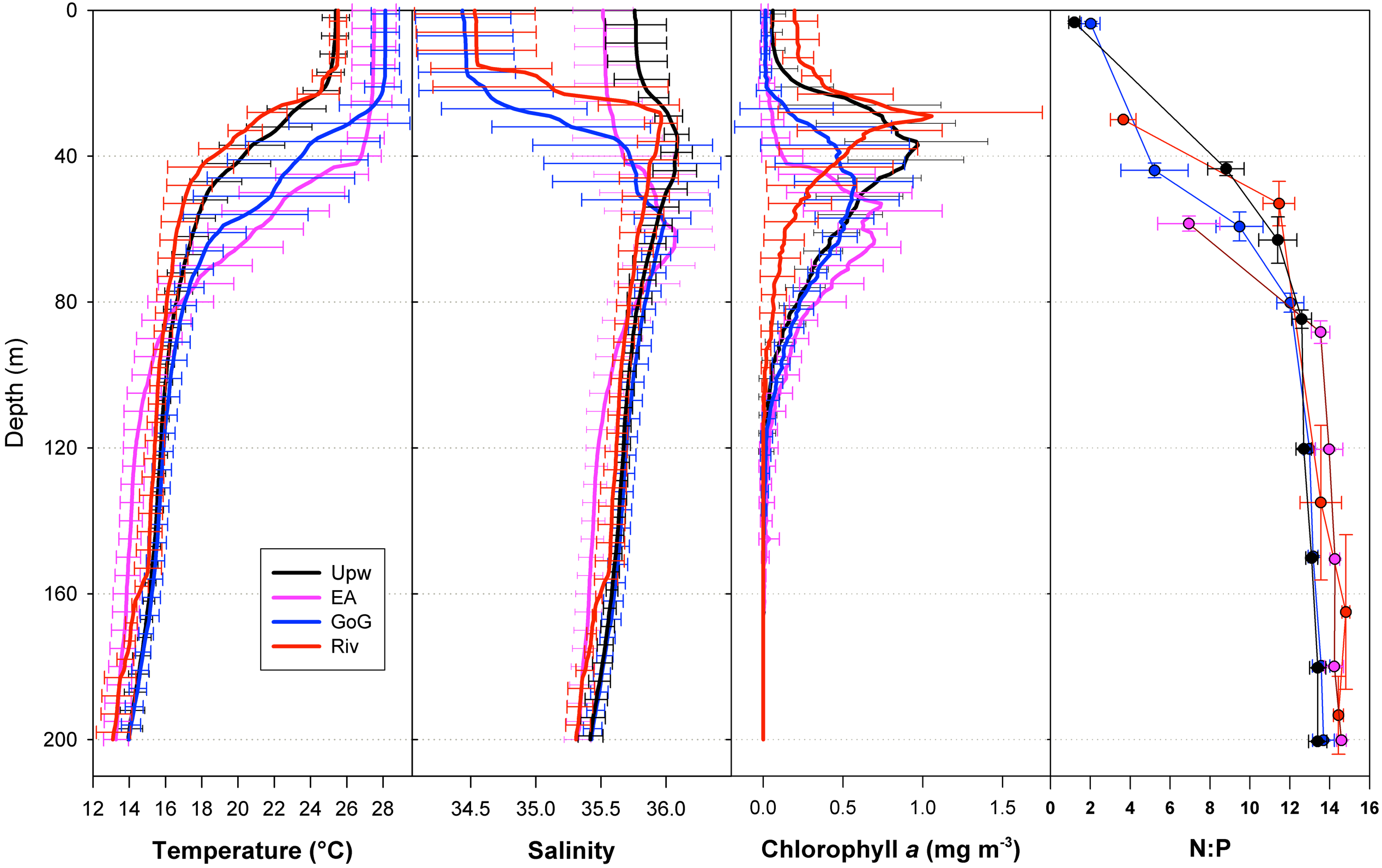
Depth (m)
0
40
80
120
160
200
Upw
EA
GoG
Riv
12 14 16 18 20 22 24 26 28
Temperature (°C)
34.5 35.0 35.5 36.0
Salinity
0.0 0.5 1.0 1.5
Chlorophyll a (mg m-3)
0 2 4 6 8 10 12 14 16
N:P

Depth Integrated concentrations of chlorophyll *c* and 19'-hexanoyloxyfucoxanthin